Evaluation of surfactant nonylphenol polyethoxylated 9.5 as a corrosion inhibitor of SAE1020 steel in saline medium

Gecílio Pereira da Silva[1]*, Luiz Ferreira da Silva Filho[2], Alessandro Alisson de Lemos Araujo[3], Victor Augusto Freire Costa[4], Richelly Nayhene de Lima[5], Simone Cristina Freitas Carvalho[6],

[1] gecilio@ufersa.edu.br, [2] luiz.filho@ufersa.edu.br, [3] alessandro.lemos@ufersa.edu.br, [4] victoragusto_costa@hotmail.com, [6] simone.carvalho@ufersa.edu.br. Engineering Center, Federal Rural University of the Semiarid (UFERSA), Brazil
[5] richellylima04@gmail.com. Center of Exact and Natural Sciences, Federal Rural University of the Semiarid (UFERSA), Brazil.
* corresponding author

Abstract
Due to its relatively low cost and good chemical stability, nonylphenol polyethoxylated with an ethoxylation degree of 9.5 (NPE95) is produced on a large scale and widely used in the industry as an emulsifier, detergent, and solubilizer. Despite its extensive applicability, there is a gap in the literature regarding its corrosion inhibition properties. In this work, the surfactant NPE95 was evaluated as a corrosion inhibitor for SAE1020 steel in 3% NaCl aqueous solution, at concentrations of 5, 10 and 25 ppm. Measurements of mass loss and visual and microscopic verification of the corrosion products on the metal surface were performed through photographic records using an Olympus® SZ61 optical stereoscope and an Olympus® BX51M microscope. In addition to the previously mentioned techniques, electrochemical impedance spectroscopy (EIS) was obtained using an AUTOLAB PGSTAT 204 potentiostat/galvanostat to better confirm the surfactant's inhibitory potential. The impedance results using an inhibitor in the corrosive medium show two capacitive arcs. The first capacitive arc can be attributed to the adsorbed film on carbon steel. The second, at low frequencies, indicates a charge transfer process in the metal/electrolyte interface, or corrosion process. The ΔGads values obtained by Langmuir and El-Awady models were respectively -21.987 kJ.mol^{-1} and -10.061 kJ.mol^{-1}, indicating spontaneous physisorption processes. Data on total mass loss shows that the lowest mass loss occurred in the sample exposed to the highest surfactant concentration (25 ppm), showing a reduction of approximately 17% in the corrosion rate in the saline medium.
Keywords: adsorption; corrosion inhibitor; electrochemical impedance spectroscopy; polyethoxylated nonylphenol; surfactant;

Avaliação do surfactante nonilfenol polietoxilado 9.5 como inibidor de corrosão do aço SAE1020 em meio salino

Resumo
Devido ao seu custo relativamente baixo e boa estabilidade química, o nonilfenol polietoxilado com grau de etoxilação de 9,5 (NPE95) é produzido em larga escala e amplamente utilizado na indústria como emulsificante, detergente, solubilizante. Apesar de sua extensa aplicabilidade, existe uma lacuna na literatura a respeito de suas propriedades de inibição de corrosão. Neste trabalho, o surfactante NPE95 foi avaliado como inibidor de corrosão para o aço SAE1020 em solução aquosa de NaCl a 3%, nas concentrações de 5, 10 e 25 ppm de inibidor. Foram realizadas medições de perda de massa, verificação visual e microscópica dos produtos de corrosão na superfície do metal por meio de registros fotográficos utilizando um estereoscópio óptico Olympus® SZ61 e um microscópio Olympus® BX51M. Além das técnicas mencionadas, a espectroscopia de impedância eletroquímica (EIE) foi obtida utilizando um potenciostato/galvanostato AUTOLAB PGSTAT 204 para uma melhor confirmação do potencial inibição do surfactante. Os resultados de impedância usando o inibidor no meio corrosivo mostram duas curvas capacitivas, indicando uma maior resistência/inibição à corrosão. O primeiro arco capacitivo pode ser atribuído ao filme adsorvido no aço carbono e o segundo, em baixas frequências, indica um processo de transferência de carga na interface

metal/eletrólito, ou processo de corrosão. Os valores de ΔG_{ads} obtidos pelos modelos de Langmuir e El-Awady foram respectivamente -21,987 kJ.mol^{-1} e -10,061 kJ.mol^{-1}, indicando processos espontâneos de fissorção. Os dados sobre perda de massa total mostram que a menor perda de massa ocorreu na amostra exposta à maior concentração de surfactante (25 ppm), mostrando uma redução de aproximadamente 17% na taxa de corrosão.
Palavras-chave: *adsorção; espectroscopia de impedância eletroquímica; inibidor de corrosão; nonilfenol polietoxilado; surfactante.*

1 Introduction

Corrosion of metals causes great inconveniences and material damage in various industrial activities, with very high direct and indirect costs. These occurrences can cause downtime for maintenance and replacement of components loss of products and efficiency of production systems, and environmental contamination, among others. In extreme cases, sudden fractures of critical equipment parts can cause serious accidents including loss of human lives. The search for the development and improvement of corrosion control and combat techniques is a very current topic that has attracted the attention of many researchers (Dwivedi; Lepková; Becker, 2017; Goyal *et al*., 2018).

Carbon steel constitutes the main metallic material in mechanical construction considering its properties and its relatively low price (Dwivedi; Lepková; Becker, 2017). However, the high susceptibility to corrosive processes in different environments imposes the need to apply adequate methods of corrosion protection and control (Dwivedi; Lepková; Becker, 2017; El-Haddad *et al*., 2019; Refait *et al*., 2020). Among natural corrosive mediums, seawater is one of the most aggressive to steel, as the salts present in it accelerate the corrosive process (Refait *et al*., 2020).

The use of corrosion inhibitors to protect steels in aqueous media has been applied as a very efficient solution to minimize or even prevent corrosion when properly specified and applied. The most general classification of these inhibitors into cathodic, anodic and adsorption is made according to their protection mechanisms (Brycki *et al*., 2017). The cathodic and anodic ones form insoluble products that act as a barrier in the cathodic and anodic regions respectively and the adsorption ones are able to form protective films in the whole extension of the areas of interest, interfering in the electrochemical reactions involved (Brycki *et al*., 2017; Pedeferri, 2018). In the latter type, organic molecules with strongly polar groups are found; highlighting the surfactants. These compounds are widely used in a variety of applications due to the intrinsic character of these molecules of being able to interact with polar and non-polar substances. They are characterized by the ability to interact with oils, fats and interfaces of solutions containing solids, liquids, including water, and gases, even being capable of interacting simultaneously with both (Sarkar *et al*., 2021; Shaban; Kang; Kim, 2020; Tiwari; Mall; Solanki, 2018).

The surfactant nonylphenol polyethoxylated 9,5 (NPE95) is a non-ionic surfactant of which the hydrophobic part of the molecule comes from the nonylphenol and the hydrophilic part comes from the ethylene oxide chain (Rodrigues *et al*., 2021). Due to its relatively low cost and good chemical stability, NPE95 is produced on a large scale and widely used in the industry as an emulsifier, detergent, and solubilizer, among other things. Despite its extensive applicability, there is a gap in the literature regarding its corrosion inhibition properties.

Evaluated, in this present work, the protection efficiency of the surfactant NPE95 as a corrosion inhibitor for SAE 1020 carbon steel in 3.0% NaCl medium, using methods of electrochemical impedance spectroscopy (EIS) and mass loss.

2 Theoretical reference

2.1 Corrosion inhibitors by adsorption

Corrosion inhibitors are chemical substances designed to slow down or prevent the corrosion of metals. Some adsorption inhibitors exhibit detergent-like properties, creating space amidst impurities on the metal surface and forming a protective film. Corrosion inhibitors by adsorption are an important class in this context. They operate by forming a protective layer on the metal surface, preventing corrosive ions from coming into contact with it. This layer is formed when the inhibitor is adsorbed

onto the metal surface, creating a physical barrier that reduces the corrosion rate. The effectiveness of adsorption corrosion inhibitors depends on factors such as the nature of the inhibitor, concentration, temperature, and the agitation of the corrosive medium (Brycki *et al*., 2017).

The theoretical fractions of adsorbed molecules or degree of coverage (θ) and inhibition efficiencies (η) can be calculated from Equations 1 and 2 (Javadian; Yousefi; Neshati, 2013).

$$\theta = \frac{n\%}{100} \quad (1)$$

$$\eta\% = \frac{Rp - Rp_0}{Rp} \times 100 \quad (2)$$

where Rp is the polarization resistance of the material with the inhibitor and Rp_0 is the polarization resistance without inhibitor.

2.2 Nonylphenol polyethoxylate 9.5 (NPE95)

Nonylphenol polyethoxylate with an average number of 9.5 is a non-ionic surfactant (weight (W) = 617 g.mol^{-1}, complete solubility in water, viscosity 230-270 mPa.s at 25 °C, density 1060 kg.m^{-3}). NPE95 is a chemical compound containing a nonylphenol base with a polyethylene oxide chain that has, on average, 9.5 ethylene oxide units. This compound is commonly used in various industrial applications, including as an emulsifier, detergent, and solubilizer, among other things (Melo *et al.,* 2014).

2.3 Electrochemical impedance spectroscopy (EIS)

Electrochemical Impedance Spectroscopy (EIS) is a powerful technique for real-time evaluation of the effectiveness of corrosion inhibitors. This technique is based on the application of a small amplitude of alternating signal to an electrochemical system and the subsequent analysis of the resulting frequency response. EIS allows for the characterization of the corrosion resistance of the metallic surface and the efficiency of the corrosion inhibitor. Parameters obtained from EIS measurements include polarization resistance (R_p), electric double-layer capacitance (C_p), and the time constant associated with the inhibitor adsorption processes. These parameters provide crucial information regarding how the inhibitor acts on the metal surface and its influence on the corrosion rate (Ribeiro; Souza; Abrantes, 2015).

Polarization resistance can be assessed from the Nyquist diagram, which consists of a scatter plot in the complex plane, where the real part of impedance (resistance) is plotted on the horizontal axis (Z') and the imaginary part (reactance) is plotted on the vertical axis (Z"). After constructing the Nyquist diagram, extrapolation is performed from the right-hand side of the semicircle until it intersects the horizontal axis. The diameter of the semicircle represents the charge transfer resistance (R_t), which is equivalent to the polarization resistance (R_p). Thus, the larger the diameter of this semicircle, the higher the R_p resistance and, consequently, the lower the corrosion rate (CR) (Ribeiro; Souza; Abrantes, 2015).

3 Experimental

The evaluation of the inhibitory action of the NPE95 on SAE 1020 steel in 3.0% NaCl medium was made with data obtained from electrochemical impedance spectroscopy (EIS) analysis. It used an AUTOLAB PGSTAT 204 potentiostat/galvanostat, from Methron Autolab®, and the NOVA software version 2.0 for the acquisition and treatment of the parameters obtained. The tests were performed at open circuit potential, at room temperature, with a frequency range from 10 kHz to 4 MHz, amplitude of 0.01 V and potential stabilization time of 10 minutes before the beginning of each experiment to reach the steady state open circuit potential. The experiments were carried out in a conventional electrochemical cell with a capacity of 80.0 mL, composed of three electrodes: Ag(s)|AgCl(s)|Cl-(aq.,[Cl-]) as a reference; platinum plate with an approximate geometric area of 2.0 cm² as counter

electrode and a SAE1020 steel disk with an exposed circular surface area of approximately 1.0 cm² as working electrode. A Faraday's cage was used for the obtention of the impedance diagrams.

Before the tests, the working electrodes were submitted to polishing with silicon carbide paper in decreasing granulation of 320, 400, 500 and 1200 mesh. The polished electrodes were washed in an ultrasonic bath using bidistilled water and acetone. The experiments were performed by adding sufficient amounts of to the corrosive medium to promote concentrations of 5.0, 10.0 and 25.0 ppm and for comparison purposes, analyses were also carried out without the addition of surfactant.

The polarization resistances (R_p) obtained via EIS and the surfactant concentrations in the corrosive media were used in the construction of the adsorption curves. Through linear regression, the correlation coefficients (R^2) were obtained and used as a criterion to select the most acceptable adsorption isotherm models (Arellanes-Lozada *et al.*, 2018; Farsak; Keles; Keles, 2015). The theoretical fractions of adsorbed molecules or degree of coverage (θ) and inhibition efficiencies (η) were then calculated from Equations 1 and 2.

The spontaneity of the surfactant adsorption processes on the steel surface was calculated for each experiment, obtaining the free adsorption energies ΔGads (kJ.mol^{-1}) from Equation 3 (Javadian; Yousefi; Neshati, 2013):

$$K_{ads} = \left(\frac{1}{55{,}5}\right) \exp\left(\frac{\Delta G_{ads}}{RT}\right) \quad (3)$$

where T is the absolute temperature and R is the gas constant and K_{ads} is the equilibrium adsorption constant of the evaluated isotherm models.

In order to confirm the results obtained by EIS, it was also sought to evaluate the corrosion-inhibiting action of NPE95 by the mass loss method. These experiments were performed in duplicate, following the NACE RP0775, NACE TM169 and ASTM G1 standards (ASTM International, 1999; Bajares; Mella, 2015; NACE International, 1999). The specimens used were SAE 1020 carbon steel coupons® from Roxar Flow Measurement AS®, in the shape of a disk and with a central hole, as shown in Figure 1.

Figure 1 – Typical images of coupons utilized in mass loss corrosion tests obtained with 8 times magnification

Source: authors' archive

The sizing to obtain the diameters of the disks, holes and thicknesses was made using a digital calliper with a precision of 0.01 mm, Mitutuoyo® Absolute Digimatic model. Weighings were performed on an Ohaus® Adventurer model analytical balance with an accuracy of four decimal places. Images of the longitudinal and transversal sections were obtained with an optical stereoscope model Olympus® SZ61, with a magnification of 8 times. The initial masses and dimensions of the coupons are shown in Table 1.

Table 1 - Coupon data: initial mass and dimensions of the exposed area

Description	Mass (g)	Dimensions (mm)	Height (mm)	Exposed area (mm^2)
Absence of sufactant	20.5726	Φ = 32.13 Φ_{fM} = 17.50 Φ_{fm} = 9.95	4.05	1950.81

Solution with 5ppm (1)	20.8614	Φ = 32.10 Φ_{fM} = 17.57 Φ_{fm} = 9.99	4.13	1956.886
Solution with 5ppm (2)	20.6960	Φ = 32.10 Φ_{fM} = 17.52 Φ_{fm} =10.03	4.10	1952.249
Solution with 10ppm (1)	20.7865	Φ = 32.11 Φ_{fM} = 17.48 Φ_{fm} =9.99	4.09	1953.090
Solution with 10ppm (2)	20.7532	Φ = 32.09 Φ_{fM} = 17.10 Φ_{fm} =10.01	4.09	1952.021
Solution with 25ppm (1)	20.4470	Φ = 32.06 Φ_{fM} = 17.51 Φ_{fm} =9.97	4.06	1943.742
Solution with 25ppm (2)	20.6760	Φ = 32.12 Φ_{fM} = 17.13 Φ_{fm} =9.95	4.02	1947.276

Nota: Φ = disc diameter, Φ_{fM} = largre diameter, Φ_{fm} = smaller diameter.
(1) First sample; (2) Second sample
Source: research data

The coupons were submitted to the same test conditions used in the EIS analyses, for a period of eight weeks, 1344 hours of exposure in immersion cells in total, as shown in Figure 2. At intervals of eight days (192 hours), they were removed and subjected to chemical pickling in Clarke's solution, at room temperature, until the complete removal of the oxidation products and residues adhered. Then they were dried and weighed. Mass variations obtained in each weighing in the respective time intervals represent the corrosion rate.

Figure 2 – Immersion cells used in the tests to determine mass loss. a) Beginning of the experiments. b) 1344 hours of immersion

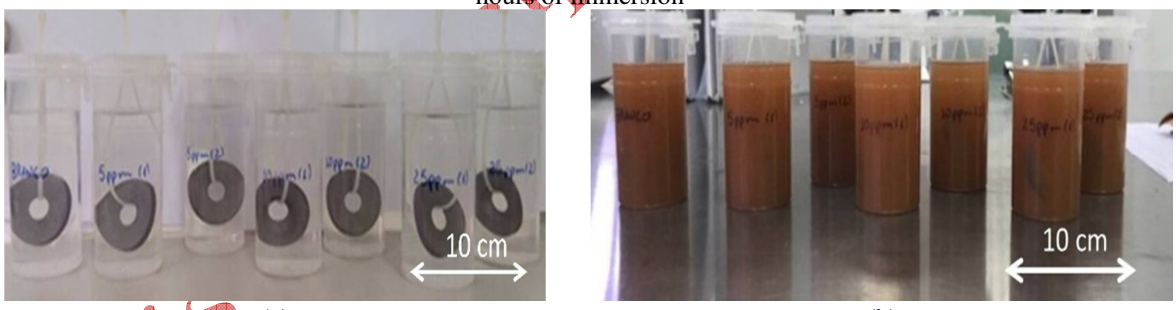

(a) (b)

Source: authors' archive

The average corrosion rates (CR) in mm year^{-1} and the inhibition efficiencies (Ef) were determined using, respectively, Equations 4 and 5 (Abdallah *et al.*, 2018; Khaksar; Shirokoff, 2017) and the qualitative classification of the corrosion rate is shown in Table 2.

$$CR = \frac{W \times 3{,}65.10^5}{A \times T \times D} \quad (4)$$

where W is the bass loss (g); A is the initial exposed area (mm^2); T is the exposure time (days) and D is the metal density (g/cm^3).

$$Ef = \frac{CR_S - CR_C}{CR_S} \; x \; 100\% \quad (5)$$

where CR_S is the corrosion rate without an inhibitor (mm/year) and CR_C is the corrosion rate with an inhibitor (mm/year).

Table 2 – Qualitative rating of uniform corrosion rate on coupons

Corrosion rate	(mm/year)
Low	< 0.025
Moderate	0.025-0.12
High	0.13-0.25
Severe	> 0.25

Source: Islam, M. *et al*. (2016)

3 Results and discussion

Figure 3 shows the Nyquist diagrams obtained, these data were used to evaluate the SAE1020 corrosion inhibition by NPE95 at the concentrations of the surfactant initially established.

Figure 3 – Electrochemical impedance diagrams of steel (SAE) 1020 in 3.0% NaCl medium, with and without the addition of NPE95

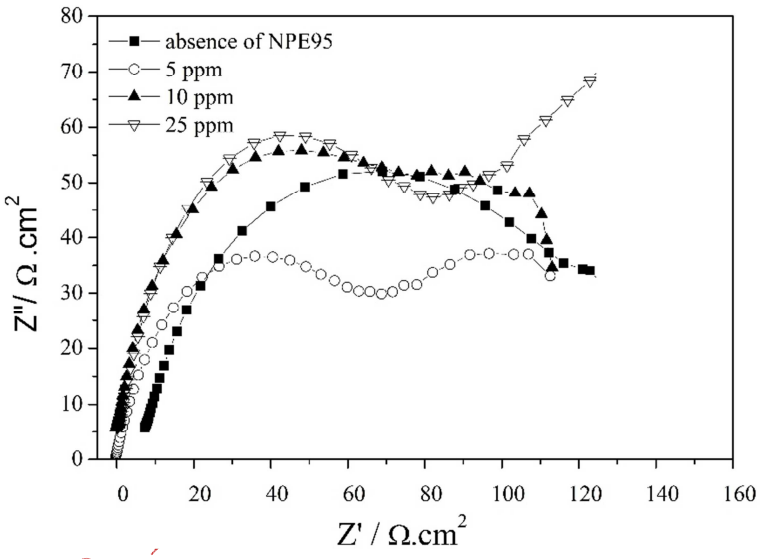

Source: research data

It is observed that the diagram generated in the absence of surfactant exhibits a single capacitive arc, characterizing a single charge transfer process, with total impedance associated with the corrosion resistance of the evaluated steel, in the saline solution, without evidence of passivation film formation. The other diagrams obtained through the addition of the surfactant in the corrosive medium show two capacitive arcs, indicating a greater inhibition of corrosion. The first capacite arc can be attributed to the adsorbed film on carbon steel. The second, at low frequencies, indicates a charge transfer process in the metal/electrolyte interface, or corrosion process. There is also an increase in the first capacitive arc total resistance with the increase of the surfactant concentration. This fact is possibly associated with the adsorption of the surfactant to the surface of the working electrode, which increases with the increase of its concentration in the medium (Abdallah *et al*., 2018; Fouda *et al*., 2019).

Table 3 presents the polarization resistance (R_p) obtained by electrochemical circle fit and the adsorbed efficiency (θ), also known as the degree of coverage. The increase in the concentration of the surfactant NPE95 effectively promoted increasing inhibition of the corrosive processes, characterized by the elevation of the total impedance modulus. In works that involve this theme, such behavior has been observed and highlighted as relevant. A typical example is presented by Torres *et al*. (2016) where a correlation was noticed between concentrations of the inhibitor present in the electrolytic

medium and the corrosion rate of the SAE 1020 carbon steel, under conditions similar to those used in this present study.

Table 3 – Experimental data of Rp for each concentration and adsorption efficiencies (θ ×100%)

Sufactant concentration (ppm)	Rp (Ω)	Adsorbed molecules efficiency (θ) (%)
0	129.75	0.00
5	132.18	13.76
10	165.68	22.79
25	166.34	25.64

Source: research data

The adsorption curves shown in Figures 4 and 5 were made from the experimental data on Rp obtained from the impedance diagrams and the fractions of molecules adsorbed on the surface (θ). The curve behavior generated from these data was compared with the following adsorption isotherm models cited in the literature: Langmuir, Temkin, Flory-Huggins and El-Awady (Foo; Hameed, 2010).

Figure 4 – Langmuir adsorption curve

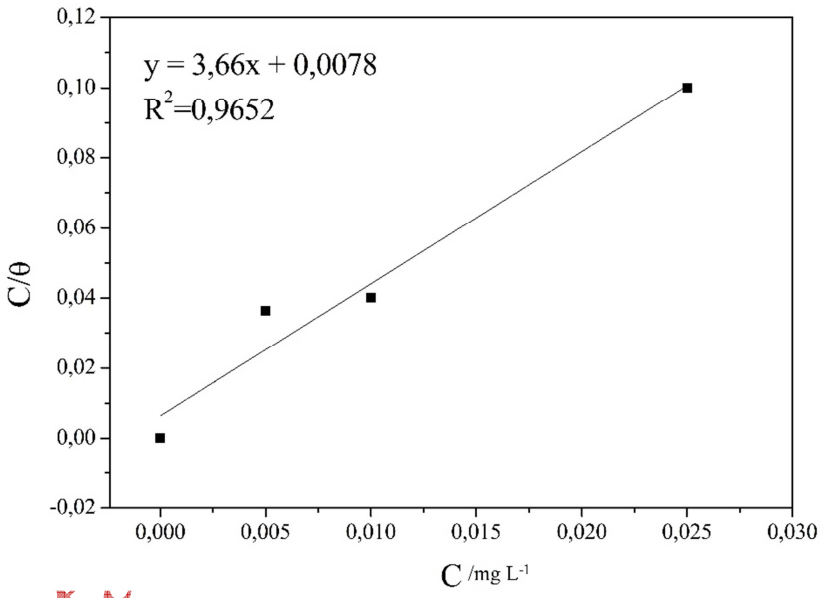

Source: research data

Figure 5 – El-Awady adsorption curve

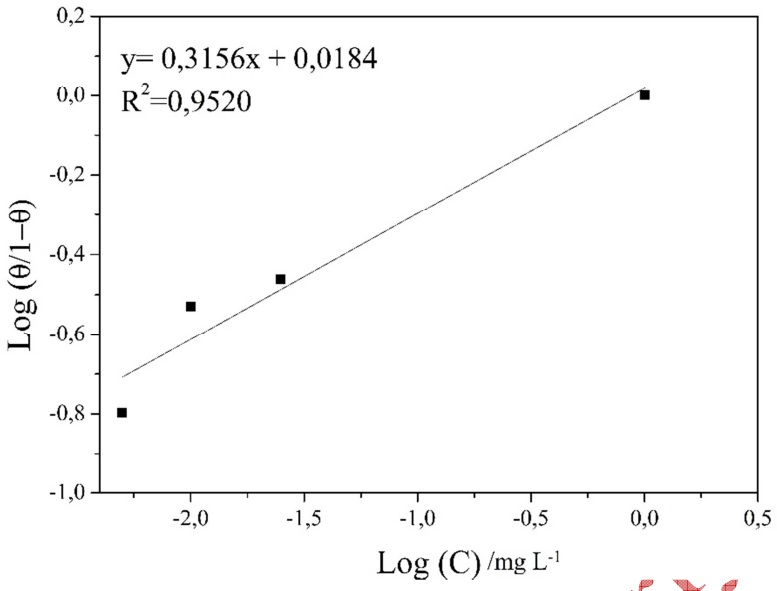

Source: research data

The Langmuir and El-Awady models shown in Figures 4 and 5, represented by Equations 6 and 7, respectively, present the best correlation coefficients R², 0.9652 and 0.9520 respectively, which the literature has already considered to be good adjustments, as demonstrated by Boulinguiez, Cloirec and Wolbert (2008).

$$C/\theta = 1/Kads + C \quad (6)$$

$$log[\theta\ /\ (1-\theta)] = log\ Kads + y\ log\ C \quad (7)$$

where C is the inhibitor concentration in mg L^{-1} ; K is the adsorption constant; θ is the fraction of molecules adsorbed on the surface and y is the number of inhibitor molecules adsorbed at an active site. From equation 3, the ΔG_{ads} values obtained by Langmuir and El-Awady models were respectively -21.987 kJ mol^{-1} and -10.061 kJ mol^{-1}, indicating spontaneous adsorption processes in the studied medium. According to Javadian, Yousefi and Neshati (2013), the energy values of ΔG_{ads} around less negative than −20 kJ mol^{-1} are associated with physisorption.

Data on total mass loss and inhibition efficiencies after the exposure of the coupons to the corrosive media are shown in Table 4. The data demonstrate that the presence of NPE95 generates a decrease of approximately 17% in the corrosion rate of steel in saline environments. Although, an increase in the concentration of NPE95 from 5 to 25 ppm does not generate a significant increase in the efficiency of the inhibitor. Thus, it can be inferred that the surfactant used in the study inhibited the corrosion process.

Table 4 – Relative mass losses and inhibition efficiencies of the NPE95 in 3% NaCl medium, at concentrations of 5.0; 10.0 and 25 ppm, and in the absence of the NPE95, at room temperature

NFP95 concentration (ppm)	Relative mass loss (%)	Inhibition efficiencies (Ef) (%)
0	0.9702	-
5	0.8571	11.00
10	0.8312	13.58
25	0.8069	16.65

Source: research data

Figure 6 shows the relative mass losses of the coupons with time of exposure to the corrosive medium. As expected, and in agreement with the results obtained via EIS, there is a tendency towards

greater losses in the absence of the surfactant, with a decrease as its concentration increases in the medium. However, as these are relative losses of mass, the differences become subtle regardless of the presence and concentration of NPE95, and identical behaviors are observed with time, which indicates a reduction only in the kinetics of the processes without major changes in the corrosion mechanisms (Torres et al., 2016; Zhu; Free, 2015).

Figure 6 – Coupons relative mass losses behavior with time in 3.0% NaCl medium in the presence of the NPE95 at concentrations of 5.0; 10.0 and 25.0 ppm, and in the absence of the NPE95, at room temperature

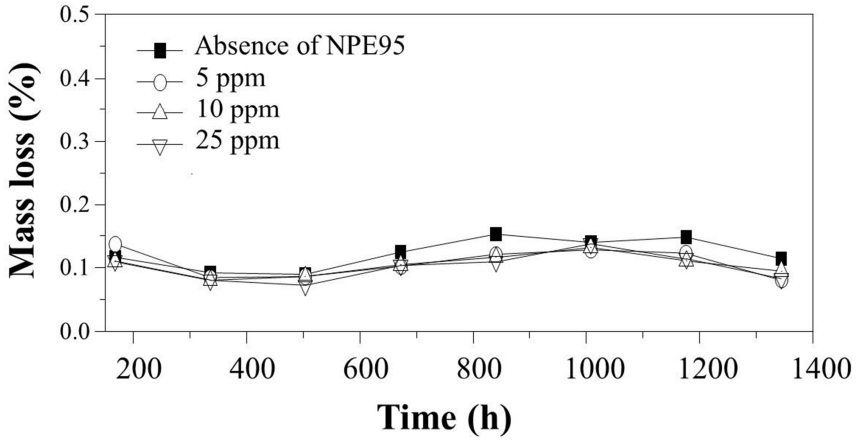

Source: research data

Figure 7 shows the influence of inhibitor concentration on the average corrosion rate over the 1344 hours interval. Values were determined considering the specific mass of the SAE 1020 steel (7.85g.cm^{-3}), mass losses of each electrode and the respective exposed areas. The curve behavior demonstrates that the corrosion rate decreases while the surfactant concentration increases, in agreement with the results observed previously. Corrosion rates in all specimens were considered moderate, according to NACE RP0775 (International, 1999).

Figure 7 – Corrosion rate of the coupons determined in the period of 1344 hours of exposure in 3.0% NaCl medium

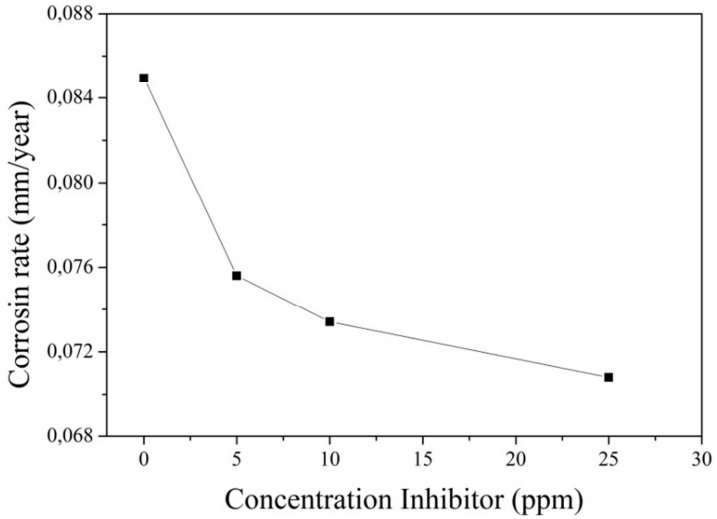

Source: research data

4 Conclusion

The experimental results showed that the surfactant nonylphenol polyethoxylated with a degree of ethoxylation of 9.5 promoted corrosion inhibition on 1020 steel in the studied medium. These results were verified by both techniques used in the study.

The impedance results using an inhibitor in the corrosive medium show two capacitive arcs. The first capacitive arc can be attributed to the adsorbed film on carbon steel. The second, at low frequencies, indicates a charge transfer process in the metal/electrolyte interface, or corrosion process. The increase in the concentration of the surfactant NPE95 effectively promoted increasing inhibition of the corrosive processes, characterized by the elevation of the total impedance modulus.

Data on total mass loss demonstrate that the presence of NPE95 generates a decrease of approximately 17% in the corrosion rate of steel in saline environments.

From this perspective, it can be inferred that NPE95 demonstrates its potential as a corrosion inhibitor for steels in a saline medium. However, further research involving higher concentrations of NPE95 or its combination with other additives may yield even more superior corrosion inhibition data in a saline medium.

Financial support

There has been no significant financial support for this work that could have influenced its outcome.

Conflicts of interest

We have no conflicts of interest to disclose.

References

ABDALLAH, M.; HEGAZY, M. A.; ALFAKEER, M.; AHMED, H. Adsorption and inhibition performance of the novel cationic Gemini surfactant as a safe corrosion inhibitor for carbon steel in hydrochloric acid. **Green Chemistry Letters and Reviews,** v. 11, n. 4, p. 457-468, 2018. DOI: https://doi.org/10.1080/17518253.2018.1526331.

ARELLANES-LOZADA, P.; OLIVARES-XOMETL, O.; LIKHANOVA, N. V.; LIJANOVA, I. V.; VARGAS-GARCÍA, J. R.; HERNÁNDEZ-RAMÍREZ, R. E. Adsorption and performance of ammonium-based ionic liquids as corrosion inhibitors of steel. **Journal of Molecular Liquids**, v. 265, p. 151-163, 2018. DOI: https://doi.org/10.1016/j.molliq.2018.04.153.

ASTM International – American Society for Testing and Materials. **ASTM G1-03(2017)e1**. Standard practice for preparing, cleaning, and evaluation corrosion test specimens. 1999.

BAJARES, R. A; MELLA, L. Study of the corrosion rate in the couple of steels ASTM A-36 and AISI / SAE 304 in a water-coke of petroleum system . **Procedia Materials Science**, v. 8, p. 702-711, 2015. DOI: http://dx.doi.org/10.1016/j.mspro.2015.04.127.

BOULINGUIEZ, B.; CLOIREC, P.; WOLBERT, D. Revisiting the determination of Langmuir parameters-application to tetrahydrothiophene adsorption onto activated carbon. **Langmuir**, v. 24, n. 13, p. 6420-6424, 2008. DOI: https://doi.org/10.1021/la800725s.

BRYCKI, B. E.; KOWALCZYK, I. H.; SZULC, A.; KACZEREWSKA, O.; PAKIET, M.; Organic corrosion inhibitors. *In*: ALIOFKHAZRAEI, M. (ed.). **Corrosion inhibitors, principles and recent applications**. 2017. p. 3-34. Available at: https://www.intechopen.com/chapters/58695. Accessed on: 09 out. 2023.

DWIVEDI, D.; LEPKOVÁ, K.; BECKER, T. Carbon steel corrosion: a review of key surface properties and characterization methods. **RSC Advances**, v. 8, p. 4580-4610, 2017. DOI: https://doi.org/10.1039/C6RA25094G.

EL-HADDAD, M. A M.; RADWAN, A. B.; SLIEM, M. H.; HASSAN, W. M. I.; ABDULLAH, A. M. Highly efficient eco-friendly corrosion inhibitor for mild steel in 5 M HCl at elevated temperatures: experimental & molecular dynamics study. **Scientific Reports**, n. 9, 3695, p. 1-15, 2019. DOI: http://dx.doi.org/10.1038/s41598-019-40149-w.

FARSAK, M.; KELES, H.; KELES, M. A new corrosion inhibitor for protection of low carbon steel in HCl solution. **Corrosion Science**, v. 98, p. 223-232, 2015. DOI: https://doi.org/10.1016/j.corsci.2015.05.036.

FOO, K Y; HAMEED, B H. Insights into the modeling of adsorption isotherm systems. **Chemical Engineering Journal**, v. 156, n. 1, p. 2-10, 2010. DOI: https://doi.org/10.1016/j.cej.2009.09.013.

FOUDA, A. S.; EL-ASKALANY, A T; EL-HABAB, A. T.; AHMED, S. Anticorrosion properties of some nonionic surfactants on carbon steel in 1 M HCl environment. **Journal of Bio- and Tribo-Corrosion**, v. 5, n. 3, p. 1-14, 2019. DOI: https://doi.org/10.1007/s40735-019-0248-2.

GOYAL, A.; POUYA, H. S.; GANJIAN, E.; CLAISSE, P. A review of corrosion and protection of steel in concrete. **Arabian Journal for Science and Engineering**, v. 43, p. 5035-5055, 2018. DOI: https://doi.org/10.1007/s13369-018-3303-2.

JAVADIAN, S.; YOUSEFI, A.; NESHATI, J. Synergistic effect of mixed cationic and anionic surfactants on the corrosion inhibitor behavior of mild steel in 3.5% NaCl. **Applied Surface Science**, v. 285, n. Part B, p. 674-681, 2013. DOI: http://dx.doi.org/10.1016/j.apsusc.2013.08.109.

KHAKSAR, L.; SHIROKOFF, J. Effect of elemental sulfur and sulfide on the corrosion behavior of cr-mo low alloy steel for tubing and tubular components in oil. **Materials**, v. 10, n. 4, 430, 2017. DOI: https://doi.org/10.3390/ma10040430.

MELO, R. P. F.; BARROS NETO, E. L.; MOURA, M. C. P. A.; DANTAS, T. N. C.; DANTAS NETTO, A. A.; OLIVEIRA, H. N. M. Removal of reactive blue 19 using nonionic surfactant in cloud point extraction. **Separation and Purification Technology**, v. 138, p. 71-76, 2014. DOI: https://doi.org/10.1016/j.seppur.2014.10.009.

NACE INTERNATIONAL – NATIONAL ASSOCIATION OF CORROSION ENGINEERS. **Standard Recommended Practice**: Preparation, installation, analysis, and interpretation of corrosion coupons in oilfield operations, 1999.

PEDEFERRI, P. Cathodic and anodic protection. *In*: Corrosion Science and Engineering. **Springer**, 2018. p. 383-422. DOI: https://doi.org/10.1007/978-3-319-97625-9_19.

REFAIT, P.; GROLLEAU, A.-M.; JEANNIN, M.; RÉMAZEILLES, C.; SABOT, R. Corrosion of carbon steel in marine environments: role of the corrosion product layer. **Corrosion and Materials Degradation Review**, v. 1, n. 1, p. 198-218, 2020. DOI: https://doi.org/10.3390/cmd1010010.

RIBEIRO, D. V.; SOUZA, C. A. C.; ABRANTES, J. C. C. Use of Electrochemical Impedance Spectroscopy (EIS) to monitoring the corrosion of reinforced concrete. **Revista IBRACON de Estruturas e Materiais**, v. 8, n. 4, p. 529-546, 2015. DOI: https://doi.org/10.1590/S1983-41952015000400007.

RODRIGUES, F. M. A.; ARRUDA, G. M.; SILVA, D. C.; COSTA, F. M. F.; BRITO, M. F. P.; ANTONINO, A. C. D.; WANDERLEY NETO, A. O. Application of nonionic surfactant nonylphenol

to control acid stimulation in carbonate matrix. **Journal of Petroleum Science and Engineering**, v. 203, 108654, p. 1-8, 2021. DOI: https://doi.org/10.1016/j.petrol.2021.108654.

SARKAR, R.; PAL, A.; RAKSHIT, A.; SAHA, B. Properties and applications of amphoteric surfactant: a concise review. **Journal of Surfactants and Detergents**, v. 24, n. 5, p. 709-730, 2021. DOI: https://doi.org/10.1002/jsde.12542.

SHABAN, S. M.; KANG, J.; KIM, D.-H. Surfactants: recent advances and their applications. **Composites Communications**, v. 22, 100537, 2020. DOI: https://doi.org/10.1016/j.coco.2020.100537.

TIWARI, S.; MALL, C.; SOLANKI, P. P. Surfactant and its applications: a review. **International Journal of Engineering Research and Application**, v. 8, n. 9, p. 61-66, 2018. Disponível em: https://www.ijera.com/papers/vol8no9/p1/M0809016166.pdf. Acesso em: 25 mar. 2022.

TORRES, V. V.; CABRAL, G. B.; SILVA; A. C. G.; FERREIRA, K. C. R.; D'ELIA, E. Ação inibidora de extratos da semente do mamão papaia na corrosão do aço-carbono 1020 em HCl 1 mol.L^{-1}. **Quimica Nova**, v. 39, n. 4, p. 423-430, 2016. DOI: https://doi.org/10.5935/0100-4042.20160046.

ZHU, Y.; FREE, M. L. Experimental investigation and modeling of the performance of pure and mixed surfactant inhibitors: micellization and corrosion inhibition. **Colloids and Surfaces A: Physicochemical and Engineering Aspects**, v. 489, p. 407-422, 2015. DOI: http://dx.doi.org/10.1016/j.colsurfa.2015.11.005.